J|A|C|S
ARTICLES
Published on Web 02/11/2003

Characterization of Electronic Structure and Properties of a Bis(histidine) Heme Model Complex

Dayle M. A. Smith, Michel Dupuis, Erich R. Vorpagel, and T. P. Straatsma*

Contribution from the Environmental Molecular Sciences Laboratory, Pacific Northwest National Laboratory, Richland, Washington 99352

Received August 7, 2002; E-mail: tps@pnl.gov

Abstract: Ferric and ferrous hemes, such as those present in electron transfer proteins, often have low-lying spin states that are very close in energy. To explore the relationship between spin state, geometry, and cytochrome electron transfer, we investigate, using density functional theory, the relative energies, electronic structure, and optimized geometries for a high- and low-spin ferric and ferrous heme model complex. Our model consists of an iron-porphyrin axially ligated by two imidazoles, which model the interaction of a heme with histidine residues. Using the B3LYP hybrid functional, we found that, in the ferric model heme complex, the doublet is lower in energy than the sextet by 8.4 kcal/mol and the singlet ferrous heme is 6.7 kcal/mol more stable than the quintet. The difference between the high-spin ferric and ferrous model heme energies yields an adiabatic electron affinity (AEA) of 5.24 eV, and the low-spin AEA is 5.17 eV. Both values are large enough to ensure electron trapping, and electronic structure analysis indicates that the iron d_π orbital is involved in the electron transfer between hemes. Mössbauer parameters calculated to verify the B3LYP electronic structure correlate very well with experimental values. Isotropic hyperfine coupling constants for the ligand nitrogen atoms were also evaluated. The optimized geometries of the ferric and ferrous hemes are consistent with structures from X-ray crystallography and reveal that the iron−imidazole distances are significantly longer in the high-spin hemes, which suggests that the protein environment, modeled here by the imidazoles, plays an important role in regulating the spin state. Iron−imidazole dissociation energies, force constants, and harmonic frequencies were calculated for the ferric and ferrous low-spin and high-spin hemes. In both the ferric and the ferrous cases, a single imidazole ligand is more easily dissociated from the high-spin hemes.

Introduction

In heme proteins, at least one iron-porphyrin complex is present and is involved in the activity of the biological system. Examples include oxygen transport agents such as hemoglobin, metabolizing enzymes such as peroxidases, and electron transfer agents such as cytochromes.[1] The functions of these proteins are modulated by the oxidation state of the iron, the spin multiplicity of the ground and low lying excited states, and the nature and geometry of the axial ligands. For instance, oxygen transport heme proteins function only in a ferrous state, switching between high- and low-spin ground states, and electron transfer agents function by reversible oxidation/reduction of the ferric-ferrous state.[2] Much of the biological activity centers on the heme unit and, even more specifically, on the 3d-orbitals of the central iron atom in the complex.

Among the axial ligands found bound to iron in heme proteins are methionine, cysteine, tyrosine, and histidine. In an exhaustive search of Protein Data Bank structures, bis(histidine) hemes were found to be incorporated into many cytochrome proteins,[3] including the respiratory enzyme flavocytochrome c_3 fumarate reductase (Ifc_3) in *Shewanella frigidimarina*, which contains four such hemes. The Ifc_3 protein directly couples two-electron reduction of fumarate to succinate with one-electron reduction of the hemes. Long-range electron transfer delivers electrons, acquired at the cytoplasmic bacterial membrane, via the heme groups that are lined up as a molecular wire to the flavin adenine dinucleotide (FAD) active site where the fumarate reduction occurs. The four *c*-hemes have midpoint reduction potentials of +10, −108, −136, and −229 mV (pH 7.5),[4] where the last heme is closest to the FAD active site. The proximities of the hemes to each other and their midpoint reduction potentials indicate that the heme of lowest potential modulates the fumarate reduction rate and that the reduction potential is affected by the protein conformation, making more than one electron transfer pathway possible.[5]

The CymA and OmcA cytochromes, also found in *S. frigidamarina*, contain 4 and 10 bis-ligated *c*-hemes, respectively. Both proteins exhibit UV−vis spectra characteristic of low-spin charge transfer between porphyrin and iron.[4] This finding was further verified in the EPR spectrum of fully oxidized CymA at 10 K, which included features typical of a low-spin ($S = {}^1/_2$) ferric heme with bis-ligated histidines in a

(1) Cotton, A. C.; Wilkinson, G. *Advanced Inorganic Chemistry*, 6th ed.; John Wiley & Sons: New York, 1999.
(2) Loew, G. H.; Harris, D. L. *Chem. Rev.* **2000**, *100*, 407−419.
(3) Zaric, S. D.; Popovic, D. M.; Knapp, E. W. *Biochemistry* **2001**, *40*, 7914−7928.
(4) Field, S. J.; Dobbin, P. S.; Cheesman, M. R.; Watmough, N. J.; Thomson, A. J.; Richardson, D. J. *J. Biol. Chem.* **2000**, *275*, 8515−8522.
(5) Butt, J. N.; Thornton, J.; Richardson, D. J.; Dobbin, P. S. *Biophys. J.* **2000**, *78*, 1001−1009.

10.1021/ja0280473 CCC: $25.00

parallel orientation. High-spin ($S = {}^5/_2$) ferric heme was also detected, but at very low levels (estimated 2% of total heme).

The preferred multiplicity of hemes is determined by the nature of the iron axial ligands and results from the competition between ligand field splitting and spin pairing energy. Ferrous iron has six electrons in its 3d shell, which can adopt a low-spin configuration ($S = 0$) or a high-spin configuration ($S = 2$), which follows Hund's rule. Similarly, ferric iron's five 3d electrons can adopt $S = {}^1/_2$ or $S = {}^5/_2$ configurations. When the ligand field splitting is small, the electron pairing energy dominates, and a high-spin configuration results. Likewise, a low-spin configuration will be preferred with strong-field ligands such as histidine or imidazole. It is interesting to note that the ligand field splitting in the mono-imidazole heme is smaller and the lowest energy electronic configuration is high spin ($S = 2$) when the central iron atom is displaced from the porphyrin plane.[6]

A characteristic property of protein-bound hemes is the presence of low-lying spin states in close energetic proximity, which is consistent with our observation in this study. Because of this small energy separation between spin states, their relative ordering and their electronic properties are very sensitive to the number and nature of the axial ligands bound to the central iron, as well as their relative orientation.[7−9] In fact, the proximity of the different spin states can be essential to protein function. For instance, in the proposed enzymatic cycle of cytochrome P450, the iron starts from the resting low-spin ferric form which converts to high-spin upon substrate binding, after which one-electron reduction occurs, yielding a high-spin ferrous state.[2,10]

As a first step toward a full characterization of the redox properties of Ifc_3, we chose bis(imidazole) iron porphyrin [$FeP(Im)_2$] as our model complex. The imidazoles are representative of the histidine amino acids that bind to the heme group in Ifc_3. The net charges of the ferric and ferrous model hemes are +1 and 0, respectively. We optimized the geometries of this model system to explore the relationship between geometry and spin state in the same heme complex, particularly the influence of the axial imidazole ligands. Restricted open-shell Hartree−Fock (ROHF) geometry optimizations of $Fe(III)P(Im)(H_2O)$ performed by Loew and Dupuis[11] showed that, although the optimized structures of the high- and low-spin complexes are quite similar, the iron−imidazole ($Fe-N_\epsilon$) distances in the two complexes are different. They also observed a slight difference in the porphyrin "core size", the average distance between iron and the four porphyrin nitrogen atoms, in the different spin states. In the present work, both $Fe-N_\epsilon$ distance and core size are larger in the high-spin hemes, which indicates that the environment of the protein could modulate spin state changes by imposing geometric changes on the iron−ligand bonds.

In the present study, comparison of the relative energies and Fe(3d) orbital configurations of the different spin states of the ferric and ferrous $FeP(Im)_2$ complexes yielded a positive adiabatic electron affinity of the system and helped us gain insight into the molecular orbitals involved in the electron transfer between hemes in intact cytochromes such as Ifc_3. We also calculated Mössbauer parameters and isotropic hyperfine coupling constants to examine the influence of the porphyrin and imidazole ligands on the electronic structure of the central iron atom. We calculated harmonic frequencies and dissociation energy curves associated with the iron−imidazole bond for each of the model hemes and found that the ferrous high-spin heme more readily dissociates a single imidazole ligand than do the ferric and low-spin hemes.

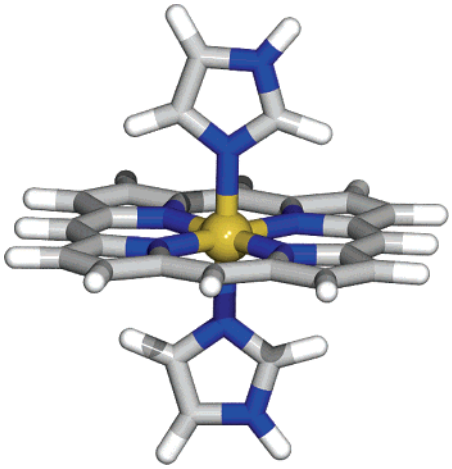

Figure 1. $FeP(Im)_2$ model heme.

Computational Methods

Our six-coordinate model heme is oriented so that the porphyrin ring is in the *xy* plane, with the nitrogen atoms on the *x*- and *y*-axes. The imidazole planes are parallel and are perpendicular to the porphyrin, bisecting its N−Fe−N angles (see Figure 1).

Experiments have shown that for low-spin ferric and ferrous hemes, parallel orientation of axial ligands was energetically favored for bulky ligands, such as substituted imidazoles, because this orientation minimizes steric interaction between imidazole hydrogen and porphyrin nitrogen atoms.[8,9,12,13] X-ray and Mössbauer experiments also demonstrated that the porphyrin ring adopts a planar configuration when bis-ligated by imidazoles in parallel planes, while imidazoles in perpendicular planes cause porphyrin ruffling.[8]

Calculations of the optimized geometries, electronic structure, and relative energies of the high- and low-spin ferric and ferrous model hemes were performed using NWChem, the software package for computational chemistry on massively parallel computers developed by the High Performance Computational Chemistry Group at the Pacific Northwest National Laboratory.[14] Calculations were performed in parallel using the IBM SP, employing up to 64 375-MHz Power3 processors.

As stated earlier in the Introduction, bis(histidine) hemes have states of different spin multiplicity in close energetic proximity. Recent studies, which compare unrestricted Hartree−Fock with DFT functionals such as B3LYP, BLYP, and Half-and-Half, provide ample

(6) Kozlowski, P. M.; Spiro, T. G.; Zgierski, M. Z. *J. Phys. Chem. B* **2000**, *104*, 10659−10666.
(7) Elkaim, E.; Tanaka, K.; Coppens, P.; Scheidt, W. R. *Acta Crystallogr., Sect. B−Struct. Commun.* **1987**, *43*, 457−461.
(8) Safo, M. K.; Gupta, G. P.; Walker, F. A.; Scheidt, W. R. *J. Am. Chem. Soc.* **1991**, *113*, 5497−5510.
(9) Safo, M. K.; Nesset, M. J. M.; Walker, F. A.; Debrunner, P. G.; Scheidt, W. R. *J. Am. Chem. Soc.* **1997**, *119*, 9438−9448.
(10) Schunemann, V.; Winkler, H. *Rep. Prog. Phys.* **2000**, *63*, 263−353.
(11) Loew, G.; Dupuis, M. *J. Am. Chem. Soc.* **1997**, *119*, 9848−9851.
(12) Walker, F. A.; Huynh, B. H.; Scheidt, W. R.; Osvath, S. R. *J. Am. Chem. Soc.* **1986**, *108*, 5288−5297.
(13) Safo, M. K.; Scheidt, W. R.; Gupta, G. P. *Inorg. Chem.* **1990**, *29*, 626−633.
(14) Harrison, R. J.; Nichols, J. A.; Straatsma, T. P.; Dupuis, M.; Bylaska, E. J.; Fann, G. I.; Windus, T. L.; Apra, E.; de Jong, W.; Hirata, S.; Hackler, M. T.; Anchell, J.; Bernholdt, D.; Borowski, P.; Clark, T.; Clerc, D.; Dachsel, H.; Deegan, M.; Dyall, K.; Elwood, D.; Fruchtl, H.; Glendening, E.; Gutowski, M.; Hirao, K.; Hess, A.; Jaffe, J.; Johnson, B.; Ju, J.; Kendall, R.; Kobayashi, R.; Kutteh, R.; Lin, Z.; Littlefield, R.; Long, X.; Meng, B.; Nakajima, T.; Nieplocha, J.; Niu, S.; Rosing, M.; Sandrone, G.; Stave, S.; Taylor, H.; Thomas, G.; van Lenthe, J.; Wolinski, K.; Wong, A.; Zhang, Z. NWChem, A Computational Chemistry Package for Parallel Computers, version 4.1; Pacific Northwest National Laboratory: Richland, Washington 99352-0999, USA, 2002.

evidence that both the sign and the magnitude of energy differences between spin states are very sensitive to the choice of functional.[2,15,16] Our experience indicates that UHF favors high-spin states, generalized gradient-corrected functionals favor low-spin states, and functionals that include a fraction of the exact exchange yield small energy differences between low- and high-spin states. (For intermediate spin states, this issue, not clearly put forth,[15] is compounded by the fact that spin contamination can be very large for some functionals and not for others, depending on the initial guess of the density and the SCF convergence method, so that results for intermediate spin states can vary widely.)[17] The sensitivity of the spin state ordering to the functionals, particularly the fraction of the exact exchange, indicates that there is no such thing as the "right" functional for predicting spin state splitting energies. For example, Scherlis and Darin[15] showed that Half-and-Half predicts the correct spin state for a pentacoordinate heme, while B3LYP works best for a closely related hexacoordinate heme. It is natural then that one might consider adjusting the mixture of correlation and exchange functionals,[18,19] to reproduce experimental data for a class of molecular systems, as has been done for chemical kinetics.[20,21] Until there are a large number of detailed comparisons with experimental energy data and a number of predictions with a high level of reliability, it will not be possible to unequivocally *predict* energy splittings for heme systems. In the present study, our aim is to calculate spin state splitting consistent with a small energy separation. Toward this end, we must turn to other criteria to judge the quality of the Kohn−Sham wave function. We will show that molecular electronic properties, such as Mössbauer quadrupole splitting, can be used for further comparison between theory and experiment. The ability of the B3LYP functional to yield Mössbauer parameters that correlate well with experimental values has already been recognized.[22,23] Our results indicate that the Mössbauer parameters for the low-spin states calculated with the B3LYP functional are in good accord with the experimentally determined data for the ground state and that, further, the same functional indicates that the low-spin state is the ground state. On that basis, and other comparisons, we expect that the B3LYP description of the system at hand is qualitatively and semiquantitatively correct, including for the aspects related to spin crossover.

We used the Ahlrich VTZ basis set for iron, and 6-311+G** for the porphyrin and imidazoles. Loew and Harris used a similar basis set for their calculations of the relative energies of low-lying iron porphyrin spin states.[2] A reasonable starting guess for the open-shell density of the model heme complex was calculated from UHF (unrestricted Hartree−Fock) orbitals of the iron, porphyrin, and imidazole fragments. The DFT initial guess for the whole system was then calculated from UHF orbitals converged from concatenated fragment orbitals.

To gain more insight into the relationship between the imidazole ligands and iron spin state, we calculated the force constants, harmonic frequencies, and dissociation energy curves associated with the Fe−N_ϵ bond for each of the model hemes. The force constants were calculated by finite difference using eight imidazole displacements of 0.03 Å from equilibrium, and the frequencies were calculated from the force constants using the reduced mass of iron-porphyrin and imidazole. The imidazole dissociation energy due to Fe−N_ϵ bond stretching was calculated for all of the model hemes, using the B3LYP functional and the same basis set as in the geometry optimizations.

(15) Scherlis, D. A.; Estrin, D. A. *Int. J. Quantum Chem.* **2002**, *87*, 158−166.
(16) Axe, F. U.; Flowers, C.; Loew, G. H.; Waleh, A. *J. Am. Chem. Soc.* **1989**, *111*, 7333−7339.
(17) Dupuis, M., unpublished results.
(18) Reiher, M.; Salomon, O.; Hess, B. A. *Theor. Chem. Acc.* **2001**, *107*, 48−55.
(19) Salomon, O.; Reiher, M.; Hess, B. A. *J. Chem. Phys.* **2002**, *117*, 4729−4737.
(20) Lynch, B. J.; Fast, P. L.; Harris, M.; Truhlar, D. G. *J. Phys. Chem. A* **2000**, *104*, 4811−4815.
(21) Lynch, B. J.; Truhlar, D. G. *J. Phys. Chem. A* **2001**, *105*, 2936−2941.
(22) Godbout, N.; Havlin, R.; Salzmann, R.; Debrunner, P. G.; Oldfield, E. *J. Phys. Chem. A* **1998**, *102*, 2342−2350.
(23) Havlin, R. H.; Godbout, N.; Salzmann, R.; Wojdelski, M.; Arnold, W.; Schulz, C. E.; Oldfield, E. *J. Am. Chem. Soc.* **1998**, *120*, 3144−3151.

Table 1. Total Energies, High-Spin/Low-Spin Relative Energies, Vertical Dissociation Energies, Adiabatic Electron Affinities, Optimized Geometries, ESP Charges, and Mulliken Charges (Parentheses) of the Model Heme Complex

	$[Fe(II)P(Im)_2]^0$		$[Fe(III)P(Im)_2]^{+1}$	
property	$S=0$	$S=2$	$S={}^1/_2$	$S={}^5/_2$
energy (hartrees)	−2705.050678	−2705.039968	−2704.860796	−2704.847378
$\Delta E_{hs/ls}$ (kcal/mol)	0.0	6.7	0.0	8.4
D_e (kcal/mol)	20.8	8.1	31.8	21.8
AEA (eV)			5.17	5.21
iron−ligand distances (Å)				
Fe−N_ϵ (calc.)	2.05	2.36	2.02	2.24
Fe−N_ϵ (exp.)	2.00[a]		1.97[b]	2.25[c]
Fe−N_{pyr} (calc.)	2.03	2.09	2.02	2.07
Fe−N_{pyr} (exp.)	2.00[a]		2.01[b]	2.05[c]
net atomic charge (electrons)				
N_{pyr}	−0.22 (−0.01)	−0.25 (−0.07)	−0.23 (−0. 01)	−0.27 (−0.04)
N_ϵ	−0.11 (−0.08)	−0.22 (−0.16)	−0.12 (−0.10)	−0.23 (−0.19)
Fe	0.49 (1.74)	0.59 (1.93)	0.68 (1.89)	0.83 (2.24)

[a] Bis(1-substituted imidazoles)(tetraphenylporphinato)iron(II) − ref 13. [b] Bis(1-methylimidazole)(*meso*-tetramesitylporphinato)iron(III) − ref 8. [c] Bis(2-methylimidazole)(octaethylporphinato)iron(III) − ref 7.

The geometry was held rigid during the bond stretching, so the dissociation energies calculated represent the vertical detachment of the imidazoles.

Quadrupole splitting measured with Mössbauer spectroscopy depends on the occupation of the Fe(3d) orbitals and the charges surrounding the central iron atom and is useful for measuring the oxidation and spin state of iron atoms in heme proteins. Theoretical verification of the Mössbauer quadrupole splitting (ΔE_Q) is an effective means of confirming the electronic environment around the iron atom. Once the geometry optimizations converged, the resulting Kohn−Sham orbitals were used to calculate the electric field gradient (EFG) tensor, which was then used to calculate Mössbauer parameters ΔE_Q and η, the asymmetry parameter. ΔE_Q and η are related to the components of the EFG tensor as follows:

$$\eta = \frac{|V_{xx} - V_{yy}|}{V_{zz}} \tag{1}$$

$$\Delta E_Q = \frac{1}{2} eQ|V_{ZZ}|\left(1 + \frac{\eta^2}{3}\right)^{1/2} \tag{2}$$

where the V values are the principal components of the EFG at the iron nucleus, e is the electron charge, and Q is the iron quadrupole moment, equal to 0.16 barn ± 5% (1 barn = 10^{-28} m^2).[24]

To examine the interaction of unpaired electrons with the s orbitals of the surrounding atoms, we also calculated isotropic hyperfine coupling constants for the ligand nitrogen atoms in our model heme according to the equation

$$A_{iso}(N) = \frac{4\pi}{3S_z}\beta_e\beta_N g_e g_N \rho_N^{\alpha-\beta} \tag{3}$$

where S_z is the z-component of the total electronic spin, β_e is the Bohr magneton, β_N is the nuclear magneton, g_e is the free electron g-value, g_N is the g-value for nucleus N, and $\rho_N^{\alpha-\beta}$ is the spin density evaluated at nucleus N.

Results and Discussion

Table 1 shows the main features of the optimized geometries obtained for the ferric hemes in doublet and sextet states and the ferrous hemes in singlet and quintet states, the total energies, the high-spin/low-spin energy differences ($\Delta E_{hs/ls}$) obtained for these states, and selected atomic Mulliken and ESP charges

(24) Dufek, P.; Blaha, P.; Schwarz, K. *Phys. Rev. Lett.* **1995**, *75*, 3545−3548.

(point charges fit to the electrostatic potential[25]). As seen from this table, the order of stability for the ferric model heme is $S = {}^1/_2 < S = {}^5/_2$. The order for the ferrous heme is $S = 0 < S = 2$ and also demonstrates that the low-spin state is energetically preferred over the high-spin state, which is consistent with predictions for the strong-field imidazole ligands.

Optimized Geometries and Net Atomic Charges. The optimized structures obtained for each spin state are very similar. The most significant differences lie in the iron−imidazole distance, Fe−N_ϵ, and the "core size", which is the average of the four iron−porphyrin nitrogen distances (although symmetry causes only two Fe−N_{pyr} distances to be unique). For each spin state species, the four Fe−N_{pyr} distances are nearly equal, with a very small pair-wise differentiation. In the ferrous hemes, the core size is larger than that in the ferric hemes to accommodate the larger ferrous ion. For both the ferric and the ferrous heme complexes, the core size is larger in the high-spin state. The distances to the axial imidazoles, which, in our model, represent the presence of the protein, differ significantly between ferric and ferrous, low- and high-spin hemes. Like the Fe−N_{pyr} bonds, the Fe−N_ϵ bonds are longer in the ferrous hemes and high-spin hemes.

The Fe−N distances in the low-spin ferrous heme and the low- and high-spin ferric hemes compare very well with those from X-ray data. The optimized geometry of the low-spin ferrous model heme is comparable to the X-ray structure of low-spin bis(1-methylimidazole)(tetraphenylporphinato) iron(II), which varied only slightly when the imidazole methyl substituent was changed.[13] The Fe−N distances in the low-spin ferric model heme are close to those measured for bis(1-methylimidazole)-(*meso*-tetramethylporphinato) iron(III)[8] and also agree well with the structures of the bis(histidine) hemes of Ifc_3. The X-ray structure for bis(2-methylimidazole)(octaethylporphinato) iron-(III)[7] contains high-spin ferric iron and correlates very well with the Fe−N bond distances in the sextet. No bis(histidine) or bis-(imidazole) hemes containing high-spin ferrous iron were found for comparison.

The ESP charges show that the charge transfer between iron and porphyrin nitrogen atoms is similar in the ferrous and ferric, high-spin and low-spin hemes, and correlates with core size. The average ESP charge for the porphyrin nitrogen atoms calculated using B3LYP/6-311+G** is $-0.51e$, which is consistent with the total porphyrin charge of -2. The charges on these atoms in the model heme system are ~ -0.25, so there is a nearly 2-fold increase due to charge transfer with the iron cation. The ESP charge for N_ϵ in an isolated imidazole, also calculated from the B3LYP/6-311+G** density, is $-0.55e$. The charge transfer between iron and imidazole is greater in the low-spin hemes because the distance to the imidazole nitrogen is shorter and is consistent with the Fe−N_ϵ overlap population (see Table 3). The net Mulliken charges are also consistent with the overlap populations and optimized geometries. The net charges on the central iron atoms are consistently lower than their formal oxidation states, which is indicative of the charge delocalization that occurs between iron and its surrounding nitrogen ligands.[26]

Iron−Imidazole Bonding. The force constants of the large-amplitude Fe−N_ϵ modes for all of the model hemes are very small (see Table 2), and the antisymmetric stretching modes are consistently smaller than the symmetric modes, which is to be expected for heavy ligands such as imidazoles. For both the ferric and the ferrous hemes, the low-spin frequencies are significantly larger than the high-spin frequencies, consistent with their shorter bond lengths and greater Fe−N_ϵ bond overlaps (see Tables 1 and 3). The low-spin harmonic frequencies are in excellent agreement with those measured for myoglobin (220 cm^{-1}) and an iron protoporphyrin IX model heme[27] (211 cm^{-1}). The ferrous harmonic frequencies are in very good agreement with the 217 cm^{-1} Fe−His Raman band observed for human liver oxygenase[28] and those calculated by Kozlowski and co-workers for pentacoordinate FeP(Im), which were 227 cm^{-1} for the singlet and 160 cm^{-1} for the quintet.[6]

Figure 2 shows the energy of dissociating a single imidazole from our $FeP(Im)_2$ model complex. It is clear from these plots that the imidazole will more readily dissociate in the high-spin

Table 2. Force Constants and Harmonic Frequencies for the $FeP(Im)_2$ Model Heme Fe−Im Symmetric and Antisymmetric Stretching Modes

	$[Fe(II)P(Im)_2]^0$		$[Fe(III)P(Im)_2]^{+1}$	
property	$S = 0$	$S = 2$	$S = {}^1/_2$	$S = {}^5/_2$
k_{sym} (kcal/mol Å^2)	381	123	483	239
ν_{sym} (cm^{-1})	213	121	239	169
k_{anti} (kcal/mol Å^2)	291	109	366	196
ν_{anti} (cm^{-1})	186	114	209	153

Table 3. Fe(3d) Population, Fe(3d) Spin Population (in Parentheses), Fe−N Overlap Population, ^{57}Fe Mössbauer Parameters, Ligand Nitrogen Isotropic Hyperfine Coupling Constants, and Spin Densities (in Parentheses)

	$[Fe(II)P(Im)_2]^0$		$[Fe(III)P(Im)_2]^{+1}$	
property	$S = 0$	$S = 2$	$S = {}^1/_2$	$S = {}^5/_2$
Fe(3d) orbital populations				
$n(d_{xy})$	1.92 (0.00)	0.99 (0.97)	1.91 (0.04)	1.01 (0.98)
$n(d_{xz})$	1.82 (0.00)	1.42 (0.53)	1.51 (0.45)	1.08 (0.91)
$n(d_{yz})$	1.82 (0.00)	1.42 (0.53)	1.48 (0.47)	1.08 (0.90)
$n(d_{x^2-y^2})$	0.45 (0.00)	1.20 (0.83)	0.65 (0.05)	1.35 (0.70)
$n(d_{z^2})$	0.40 (0.00)	1.10 (0.90)	0.66 (0.02)	1.26 (0.77)
n_d	6.42 (0.00)	6.13 (3.76)	6.21 (1.03)	5.78 (4.26)
Δn_d	0.15	−0.34	0.40	0.01
overlap populations				
n (Fe−N_{pyr})	0.28	0.16	0.31	0.22
n (Fe−N_ϵ)	0.27	0.10	0.29	0.08
Mössbauer parameters				
ΔE_Q (calc.) mm/s	0.91	2.79	2.54	1.06
ΔE_Q (exp.) mm/s	0.97−1.07[a]	2.50[b]	2.28[c]	1.3[d]
η (calc.)	0.02	0.99	0.64	0.09
η (exp.)	0.0[a]	1.0[b]		
isotropic coupling (A_{iso})				
N_{pyr} (calc.) MHz		7.89 (0.10)	−7.35 (−0.02)	9.36 (0.14)
N_{pyr} (exp.) MHz			−7.4[e]	7.60,[g] 7.95[h,i]
N_ϵ (calc.) MHz		7.38 (0.09)	−9.86 (−0.03)	9.46 (0.15)
N_ϵ (exp.) MHz			−7.8,[e] 8.8[f,i]	11.46,[g] 9.31[h,i]

[a] Bis(1-substituted imidazoles)(tetraphenylporphinato)iron(II) − ref 13. [b] Chloroperoxidase − ref 31. [c] Bis(1-methylimidazole)(*meso*-tetramesitylporphinato)iron(III) − ref 8. [d] Metmyoglobin − ref 32. [e] Bis(imidazole)(tetraphenylporphinato)iron(III) − ref 33. [f] Cytochrome *c* oxidase (magnitude only) − ref 34. [g] Metmyoglobin − ref 35. [h] Aquometmyoglobin − ref 36. [i] Includes anisotropic coupling.

(25) Jensen, F. *Introduction to Computational Chemistry*; John Wiley & Sons Ltd.: West Sussex, 1999.

(26) Johansson, M. P.; Blomberg, M. R. A.; Sundholm, D.; Wilkstron, M. *Biochim. Biophys. Acta* **2002**, *1553*, 183−187.

(27) Rosca, F.; Kumar, T. N.; Ionascu D.; Ye, X.; Demidov, A. A.; et al. *J. Phys. Chem. A* **2002**, *106*, 2540−3552.

(28) Sun, J.; Loehr, T. M.; Wilks, A.; Demontellano, P. R. O. *Biochemistry* **1994**, *33*, 13734−13740.

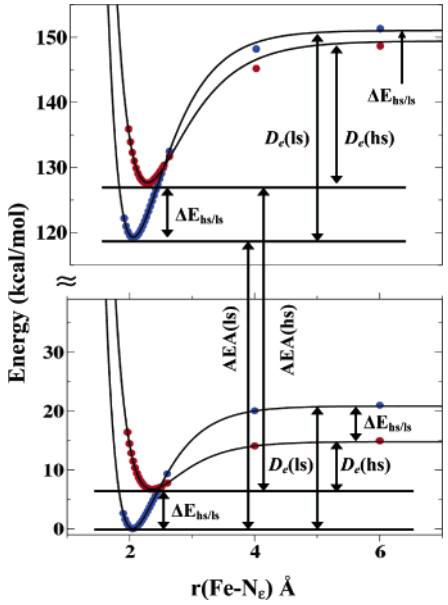

Figure 2. Energy (kcal/mol) of Fe−Im bond stretching (Å) for the low-spin (blue), high-spin (red), ferric (top), and ferrous (bottom) model hemes. The black curves are Morse potential functions fit to the dissociation potentials.

hemes, as indicated by their lower force constants. The potential wells for the ferric states are deeper than those of the ferrous states, and the potential energy curves for the high-spin ferrous and ferric states are shallower, as indicated by their dissociation energies. Vertical imidazole dissociation energies (D_e), adiabatic electron affinities (AEA), and high-spin/low-spin energy differences ($\Delta E_{hs/ls}$) for hexacoordinate FeP(Im)$_2$ are indicated on the plot and tabulated in Table 1.

In the dissociated, pentacoordinated model hemes (FeP(Im) + Im), the high-spin Fe(3d) electron configuration is preferred ($\Delta E_{hs/ls} < 0$). Although porphyrin ruffling was not allowed during the imidazole dissociation, the ferrous dissociated heme $\Delta E_{hs/ls}$ value of −6.0 kcal/mol is similar to the value of −2.9 kcal/mol reported in the literature for the pentacoordinate ferrous heme.[6]

The adiabatic electron affinity (AEA) was calculated from the energies of the ferric and ferrous hemes, each at their respective optimized geometries. For the high-spin and low-spin hemes, the AEA is 5.24 and 5.17 eV (121 and 119 kcal/mol), respectively. The positive sign and large magnitude of the AEA indicate that the bis(imidazole) hemes are effective electron traps.

Spin-Crossover. The point at which the low-spin and high-spin potentials cross, the "spin-crossover" point, occurs in the harmonic region of the Fe−Im bond stretching potential in both the ferric and the ferrous hemes. In the ferric heme, spin-crossover occurs when the iron and imidazole are 2.47 Å apart, which is at $v = 11$ in the doublet harmonic well. In the ferrous model heme, the spin-crossover occurs at 2.50 Å and $v = 12$. Thermal spin-crossover is observed when the vertical separation of zero-point energies between the high-spin and low-spin potential wells is on the order of kT,[1] which is 0.025 eV (0.6 kcal/mol) at 300 K. Differences in total energy between the high-spin and low-spin hemes (Tables 1 and 3) are sufficiently large as compared to kT that only a small fraction of molecules will populate vibrational levels at which spin-crossover can occur. Optical excitation can also induce the spin-crossover, but in a complex protein such as Ifc$_3$, an investigation into the dynamics and thermodynamics of the entire protein system is necessary to elucidate the spin-crossover behavior of these hemes. It is clear, however, that the iron−imidazole bond, which models the attachment of the heme to the protein's histidine side chains, can regulate the spin state of the iron atom. This is consistent with experimental[29] and theoretical[30] observations in iron spin-transition complexes, in which the electronic environment surrounding the central iron atom strongly influences the spin-crossover rate, low-spin/high-spin equilibrium, and spin-crossover probability.

Fe(3d) Electronic Structure. In Table 3, the Fe(3d) shell populations and spin populations, iron−ligand overlap populations, and iron Mössbauer parameters are given, as well as spin densities and isotropic hyperfine coupling constants for the ligand nitrogen atoms.

Analysis of the Mulliken Fe(3d) orbital and spin populations leads to the following electron configurations for the bis(imidazole) model hemes: $(d_{xy})^2(d_{xz})^2(d_{yz})^2$ for ferrous low-spin, $(d_{xy})^2(d_{xz},d_{yz})^3$ for ferric low-spin, $(d_{xy})^1(d_{xz},d_{yz})^3(d_{x^2-y^2})^1(d_{z^2})^1$ for ferrous high-spin, and $(d_{xy})^1(d_{xz})^1(d_{yz})^1(d_{x^2-y^2})^1(d_{z^2})^1$ for ferric high-spin. The doublet ferric and quintet ferrous hemes both utilize the degenerate $(d_{xz},d_{yz}) = d_\pi$ orbitals, which is consistent with the (π, d_π) charge transfer bands observed for low-spin ferric hemes such as cytochrome *c*[37] and high-spin ferrous heme proteins.[38] A comparison of the Fe(3d) electron configurations suggests that the d_π orbital plays an important role in the transfer of an electron between low-spin or high-spin hemes. The d_π orbital is the donor/acceptor orbital because the low-spin ferrous and ferric hemes differ in the occupancy of the degenerate d_{xz} and d_{yz} orbitals of iron, and the same can be said for the high-spin hemes. The number of electrons transferred between the Fe(3d) orbitals of the hemes is largely localized to the d_π orbitals and amounts to only 0.21 and 0.35 electrons for the low-spin and high-spin hemes, respectively, despite the unit change in oxidation state. This is due to charge delocalization between iron and the surrounding ligand nitrogens, which is reflected in the ESP charges. A recent study concluded that this delocalization is required to accommodate the heme in the low dielectric protein environment.[26] Because both low-spin and high-spin electron transfer occurs between d_π orbitals, it is not surprising that the low-spin and high-spin adiabatic electron affinities are nearly equal.

The Mössbauer parameters ΔE_Q and η depend on the EFG and reflect the spatial distribution of electrons around the iron. The EFG has two parts. The largest is a valence contribution, q_{val}, which results from the unequal electronic population of the valence orbitals, particularly the Fe(3d) orbitals. q_{val} can be

(29) Dose, E. V.; Hoselton, M. A.; Sutin, N.; Tweedle, M. F.; Wilson, L. J. *J. Am. Chem. Soc.* **1978**, *100*, 1141−1147.
(30) Gerstman, B. S.; Sungar, N. *J. Chem. Phys.* **1992**, *96*, 387−398.
(31) Champion, P. M.; Chiang, R.; Munck, E.; Debrunner, P.; L. P., H. *Biochemistry* **1975**, *14*, 4159−4166.
(32) Lang, G. *Q. Rev. Biophys.* **1970**, *3*, 1−60.
(33) Scholes, C. P.; Falkowski, K. M.; Chen, S.; Bank, S. *J. Am. Chem. Soc.* **1986**, *108*, 1660−1671.
(34) Martin, C. T.; Scholes, C. P.; Chan, S. I. *J. Biol. Chem.* **1985**, *260*, 2857−2861.
(35) Scholes, C. P.; Isaacson, R. A.; Feher, G. *Biochim. Biophys. Acta* **1972**, *263*, 448−452.
(36) Scholes, C. P.; Lapidot, A.; Mascarenhas, R.; Inubushu, T.; Isaacson, R. A.; Feher, G. *J. Am. Chem. Soc.* **1982**, *104*, 2724−2735.
(37) Du, P.; Loew, G. H. *J. Am. Chem. Soc.* **1991**, *113*, 5.
(38) Oganesyan, V. S.; Sharonov, Y. A. *Spectrochim. Acta, Part A-Molec. Biomolec. Spectrosc.* **1997**, *53*, 433−449.

described in terms of the Fe(3d) orbital anisotropy, Δn_d:[39]

$$\Delta n_d = n(d_{x^2-y^2}) + n(d_{xy}) - n(d_{z^2}) - \frac{1}{2}n(d_{xz}) - \frac{1}{2}n(d_{yz}) \quad (4)$$

The second, smaller, term is the contribution of the external lattice, q_{lat}, which contributes if the iron nucleus is in a noncubic environment. The lattice contribution can be quantitatively described by the overlap population between the iron and the imidazole or porphyrin nitrogen atoms, $n(Fe-N_\epsilon)$ and $n(Fe-N_{pyr})$. In the present study, q_{lat} will have a significant effect on the EFG and therefore the quadrupole splitting, if the $Fe-N_\epsilon$ and $Fe-N_{pyr}$ distances are significantly different. The balance of both valence and lattice effects contributes to η and V_{zz}, the largest component of the EFG, and therefore to ΔE_Q (eq 2).

In the low-spin ferrous heme ($S = 0$), all of the electrons are formally paired. The configuration of the singlet ferrous heme is $(d_{xy})^2(d_{xz})^2(d_{yz})^2$, so the electrons are evenly distributed in each direction, and the valence contribution to the electric field gradient is zero (see eq 4). The overlap with the ligand nitrogen atoms is symmetric, so the lattice contribution is also small, giving rise to the smallest quadrupole splitting of all of the hemes presented here. Our calculated Mössbauer parameters compare well with the values measured by Safo and co-workers for 1-substituted bis(imidazole) iron(II) porphyrinates at 118 K.[13]

In the high-spin ($S = 2$) ferrous heme, three Fe(3d) orbitals are singly occupied, and the d_π orbital is triply occupied. This produces an anisotropy in the *z*-direction, which contributes to the valence fraction of the EFG. The Fe−N bond overlaps are not as large as those in the $S = 0$ heme; however, there is a nearly 2-fold difference in magnitude between the iron overlaps with imidazole and porphyrin, which significantly affects the charge symmetry and therefore the lattice contribution to the EFG. In the $S = 2$ heme, valence and lattice contributions combine to yield the largest quadrupole splitting. Champion and co-workers[31] investigated the electronic structure of high-spin ferrous heme proteins and found that the quadrupole splittings for chloroperoxidase, horseradish peroxidase, hemoglobin, and cytochrome P-450 all fall in the range of 2.38−2.70 mm/s ($\eta = 0.6-1.0$), which is typical for high-spin ferrous iron.[31,40]

In the $S = {}^1/_2$ ferric model heme, the Fe(3d) orbital population differs from the $S = 0$ ferrous heme by one less d_π electron. This produces an anisotropic effect, as in the high-spin ferrous heme. There is little lattice contribution to the EFG, because the iron orbital overlap with imidazole and porphyrin nitrogen atoms is similar. Therefore, the large quadrupole splitting calculated for the low-spin ferric heme is almost entirely due to the anisotropy caused by the iron d_π orbital. Safo and co-workers[8] measured the Mössbauer spectrum of bis(1-methylimidazole)(*meso*-tetramesitylporphyrinato)iron(III), and their measured quadrupole splitting of 2.28 mm/s is in good agreement with our value.

Finally, the $S = {}^5/_2$ ferric heme, which has five electrons evenly distributed in the Fe(3d) shell, has no anisotropy and therefore no valence contribution to the EFG. The overlap between the iron and the porphyrin nitrogen atoms is nearly 3 times greater than the overlap with the imidazole, because the imidazoles are so far away. Therefore, only lattice effects contribute to the EFG, causing a small quadrupole splitting. The quadrupole splitting for metmyoglobin[32] measured by Lang at 195 K is 1.3 mm/s and is consistent with our value of 1.06 mm/s.

Hyperfine coupling constants describe the interactions of unpaired electrons with nuclei. The hyperfine interaction tensor can be factored into an isotropic component, which describes the interaction between unpaired electrons in s orbitals and nuclei, and an anisotropic component, which describes the interaction of nuclei with unpaired electrons in orbitals of higher angular momentum. Isotropic coupling constants (A_{iso}, also called Fermi contact terms) can be difficult to calculate to experimental accuracy because the spin density must be evaluated on the nuclei, where the cusps of s functions are difficult to reproduce with a Gaussian basis set. Isotropic hyperfine coupling constants and spin densities for ligand nitrogen atoms are shown in Table 3 with experimental values for low-spin and high-spin ferric hemes for comparison. Like the Mössbauer parameters, isotropic coupling constants can be explained in light of the Fe−N bond densities and Fe(3d) Mulliken spin populations.

The calculated A_{iso} values compare well with coupling constants measured using the electron nuclear double resonance (ENDOR) technique. For the doublet ferric heme, the sign and magnitude of the isotropic coupling constants are consistent with those measured for bis(imidazole) (tetraphenylporphinato) iron-(III),[33] in which the negative sign of A_{iso} was attributed to the exchange polarization of the nitrogen 2s orbitals. The N_ϵ hyperfine coupling constant measured for cytochrome *c* oxidase[34] includes both isotropic and anisotropic coupling. Comparison with the calculated isotropic coupling constants verifies that hyperfine coupling to the imidazole nitrogen is largely isotropic in the doublet ferric heme.[33]

Isotropic coupling constants measured for aquometmyoglobin[36] are comparable to our calculated values for the high-spin ferric heme, both in sign and in magnitude. The positive sign of A_{iso} has been attributed to the direct transfer of electron spin from the metal d_z^2 to the ligand nitrogen σ orbitals,[33] which is consistent with our d_z^2 orbital spin population. The nitrogen isotropic coupling constants are similar to those measured for metmyoglobin,[41] which also include anisotropic coupling, indicating that the interaction of the high-spin ferric heme's unpaired electrons with ligand nitrogen atoms is largely isotropic, as in the doublet heme.

The high-spin ferrous heme's isotropic coupling constants are also tabulated, but no experimental values were found for comparison. The positive sign is consistent with the A_{iso} values for the high-spin ferric heme. The quintet's larger core size causes the porphyrin A_{iso} to be lower in the quintet than the sextet. The lower A_{iso} on the imidazole nitrogen atom can be attributed to the longer $Fe-N_\epsilon$ distance in the high-spin ferrous heme.

Conclusions

In this study, we have shown that the B3LYP hybrid functional is effective for modeling the oxidation states and low-

(39) Grodzicki, M.; Flint, H.; Winkler, H.; Walker, F. A.; Trautwein, A. X. *J. Phys. Chem. A* **1997**, *101*, 4202−4207.
(40) Champion, P. M.; Chiang, R.; Munck, E.; Debrunner, P.; I. C., G. *Biochemistry* **1975**, *14*, 4151−4158.
(41) Mun, S. K.; Chang, J. C.; Das, T. P. *Biochim. Biophys. Acta* **1977**, *490*, 249−253.

lying spin states of bis(imidazole) hemes. The results of our geometry optimizations are in very good agreement with geometries measured for model hemes using X-ray crystallography, in which the iron−imidazole distances are significantly longer in the high-spin hemes. This indicates that a protein such as Ifc_3 can manipulate the spin state of a bis(histidine) heme by imposing geometric changes on the iron−ligand bonds.

Imidazole dissociation curves show that the spin-crossover point is similar for the ferric and ferrous hemes (∼2.5 Å) and that the ferrous and high-spin hemes dissociate a single imidazole more readily than the ferric and low-spin hemes. Both spin-crossover and imidazole dissociation are thermally inaccessible at reasonable temperatures. However, we know from studies of cytochrome P450 that the relative energies and redox properties of the heme are affected by the electric field of the protein and solvent.[42] The hydrogen bonding of hemes to residues in the distal pocket, particularly a nearby aspartate residue, and polarization by the solvent medium influence the electronic and geometric features of the heme, including axial ligand bond strength and the location of the unpaired spins.[43,44] Because our calculated geometries, Mössbauer parameters, and Fe−Im stretching frequencies correlate well with experimental results for substituted model hemes and intact heme proteins, we expect that only relative energies ($\Delta E_{hs/ls}$ and AEA) will be affected by the environment. In our next step toward a full characterization of the redox properties of Ifc_3, we will perform QM/MM calculations to explore in detail the influences of the Ifc_3 heme substituents (propionate groups, methyl groups, and attached cysteines) and the electric field due to the solvent and protein residues on the relative energies of the hemes.

Acknowledgment. The authors thank Dr. R. Kukkadapu at PNNL for sharing his expertise of Mössbauer spectroscopy, and Dr. M. Bowman at PNNL for very helpful discussions of hyperfine coupling constants. This work was supported in part by the Office of Advanced Scientific Computing Research, Office of Science, Department of Energy. Computational resources for this work were provided by the Molecular Sciences Computing Facility of the Environmental Molecular Sciences Laboratory at Pacific Northwest National Laboratory. Pacific Northwest National Laboratory is operated for the U.S. Department of Energy by the Battelle Memorial Institute.

JA0280473

(42) Loew, G. H.; Harris, D. L. *J. Am. Chem. Soc.* **1993**, *115*, 8775−8779.
(43) Ogliaro, F.; Cohen, S.; de Visser, S.; Shaik, S. *J. Am. Chem. Soc.* **2000**, *122*, 12892−12893.
(44) Green, M. T. *J. Am. Chem. Soc.* **2000**, *122*, 9495−9499.